

A Study of Reduced-Sensitivity RDX
Jimmie Oxley;* James Smith; Robert Buco; Jiaorong Huang
University of Rhode Island, Chemistry Dept
51 Lower College Road
Kingston, RI 02881
joxley@uri.edu

Abstract:

Five lots of RDX (1,3,5-trinitro-1,3,5-tri-azacyclohexane), having different sensitivities, according to Large-Scale Gap Test (LSGT) results, were studied. Laboratory investigations included direct insertion mass spectrometry, liquid chromatography, powder x-ray diffraction, polarized light with hot-stage microscopy, infrared and Raman spectroscopy, and differential scanning calorimetry (DSC). DSC proved useful at distinguishing differences between lots. The RDX lots studied included three made in the United States by BAE Ordinance Systems (Holston), one from Eurengo (formally SNPE) and one from Dyno Nobel. Of Holston RDX, two lots had been reprocessed by Eurengo to reduce sensitivity. Increased sensitivity appeared to correlate with increased HMX (octahydro-1,3,5,7-tetranitro-1,3,5,7-tetrazocine) content. Aging and heating contributed to the formation of an RDX/HMX eutectic.

Key Words:

RDX, insensitive RDX, RDX/HMX eutectic, large-scale gap test

Introduction:

In the late 1990's Eurenco (formally SNPE), reported that their RDX (1,3,5-trinitro-1,3,5-triazacyclohexane), made by the Woolwich process and a proprietary recrystallization, demonstrated special insensitivity in the Large-Scale Gap Test (LSGT). Other manufacturers (Australian Defense Industries, Royal Ordnance Defense and Dyno Nobel) later claimed similar insensitivity for their RDX. With the exception of Dyno Nobel, the others also used the Woolwich synthesis method (hexamine and nitric acid). Dyno Nobel, like RDX manufactured in the U.S. at Holston, used the Bachmann process (Type II RDX from hexamine, ammonium nitrate, acetic anhydride) which may contain 5% to 17% HMX. Dyno Nobel claimed "reduced sensitivity-RDX" was obtained with a proprietary re-crystallization process.

The U.S. Army commissioned Eurenco to transform two lots of Holston RDX into "insensitive" or "reduced sensitivity" RDX via their re-crystallization process. A concern with evaluating the different RDX lots was that insensitivity was not observed in traditional, small-scale sensitivity tests. Only in the LSGT was the sensitivity reduced (Table 1). The LSGT required that the RDX have a binder which made direct correlations with the neat RDX powders difficult to ascertain. Furthermore some studies have suggested that the Holston RDX re-crystallized by Eurenco lost its insensitivity with time. University of Rhode Island (URI) was asked to perform a number of analyses to see if the source of returned sensitivity could be determined. The samples evaluated are the same as cited in Table 1. The baseline samples are shown in Table 2.

Experimental Section:

Direct Insertion Mass Spectrometry (MS): A Finnigan MAT TSQ 700 triple stage mass spectrometer equipped with a direct insertion probe was used to collect the mass spectrum of each sample. Test solutions for samples were prepared by dissolving ~1mg of RDX in 1 mL of acetonitrile in a 2mL Agilent amber glass autosampler vial with screw cap septum. A 10 uL gas-tight syringe was used to

inject 1 μL of the solution into an aluminum sample holder, which was then placed on a sample heater block to drive off the solvent. The dried sample was inserted into the direct insertion probe and placed in the ion source of the mass spectrometer. The direct insertion probe followed a temperature program that began at 50°C and ramped at 10°C per minute to a temperature of 180°C , then by 20°C per minute to a final temperature of 300°C . Samples were analyzed in triplicate.

High Performance Liquid Chromatography (HPLC): A Hewlett Packard (now Agilent) 1100 series HPLC equipped with an Agilent Hypersil BDS-C18 column (4.00 x 100 mm) and a diode array detector tuned at 214 nm and 235 nm was used. The acquisition method was isocratic, using a 60:40 mix of water:methanol as the mobile phase at a flow rate of 0.5 mL/min. The instrument acquired data for 10 minutes, followed by a 10-minute equilibration before the next injection. Test solutions were prepared by placing ~ 10 mg of RDX in a 1 mL volumetric flask, adding of 1 μL of nitrobenzene and enough HPLC-grade acetonitrile to fill the flask. The solution was transferred into an Agilent 2 mL amber glass autosampler vial with screw-cap septum. Samples were analyzed in triplicate.

X-ray Powder Diffraction Spectroscopy (XRD): A Bruker AXS (Siemens) D5000 theta/theta X-Ray diffractometer equipped with a 40 position autosampler, a 2kW max power generator capable of 20 to 40kV and 5 to 40mA, a copper anode tube (wavelengths: $K\alpha_1$, 1.5406 \AA ; $K\alpha_2$, 1.54439 \AA ; $K\beta$, 1.39222 \AA) with average $K\alpha$ of 1.54184 \AA , K_2/K_1 ratio of 0.5 and low speed shutter, as well as a scintillation counter operating at 841.1V with an amplifier gain of 2 and 1mm, 0.1mm, 0.6mm, respectively fixed optics. Samples were gently mounded on aluminum holders and a glass slide was used to spread and level the sample. Spectra were acquired through a locked-coupled step scan between 5° and 50° by 0.020° steps at 2 seconds per step with fixed speed synchrotron rotation turned on. The power generator was run at 40KV and 40mA. Raw X-ray diffraction spectra were corrected for $K\alpha_2$ and used to compare the samples. All crystalline samples were analyzed in triplicate.

Raman Spectroscopy: A drop (5 μL) of each acetonitrile RDX solution (1000 $\mu\text{g}/\text{mL}$) was deposited, by means of a micro-pipette, onto a Tienta Sciences SpectRIM stainless steel, hydrophilic coated microscope slide. Droplets were arranged on the slide in a grid, allowing ten samples in the upper third of the slide. To reduce possible cross contamination, each droplet was allowed to dry before the next was added. A Raman spectrum of each sample was acquired using a Bruker Senterra Dispersive Raman Spectrometer interfaced to an Olympus BX51M microscope. The microscope was capable of 200x and 500x magnification and was equipped with an Infinity 1 digital camera. After aligning a sample in the view finder and capturing an image of the spot, the shielding doors around the microscope stage were closed; the shutter moved from bright field to dark; and the Raman spectrum was acquired. The laser excitation wavelength was fixed at 785nm, and the instrument was set to use a 50x1000 μm slit. Data was accumulated for 100 seconds per scan, with only one scan being reported per sample. The Raman spectra were collected in three regions, 80-1500 cm^{-1} , 1480-2600 cm^{-1} , and 2370-3280 cm^{-1} at a resolution of 3 to 5 cm^{-1} . The three regions were mathematically baseline corrected to align with each other and compiled to give the full reported Raman spectrum. Where two regions overlapped, the portion of the signal that overlapped was signal averaged to give the complete spectrum (80-3280 cm^{-1}). Original regional scans, raw data and baseline corrected, were saved in raw data format; JCAMP-DX and Galactic SPC, and compiled full range Raman spectra were recorded in the same three file formats.

Infrared Spectroscopy (IR): A SensIR Travel IR attenuated total reflectance (ATR) IR spectrometer was used to collect the IR absorbance spectrum of each sample. Samples were placed over the diamond window and subjected to 6 tons of pressure by the sample piston. Background scans (64) were collected at 4 wavenumber resolution from 4000 to 400 wavenumbers and then 64 scans of the sample under the same conditions. Samples were analyzed in triplicate.

Differential Scanning Calorimetry (DSC): A Thermal Analysis (TA) Q100 DSC equipped with a refrigerated cooling system was calibrated against zinc and indium on a weekly basis; baseline correction was calibrated each day against an empty sample pan. The acquisition program equilibrated the cell, zeroed the heat flow at 40°C, and ramped (usually by 20°C per minute) to 400°C. Samples (0.5-0.9mg) were held in hermetically sealed aluminum. Samples were analyzed in triplicate.

Polarized Light Microscopy: A Nikon E400 POL polarizing light microscope, equipped with a 5.1 Mega pixel digital camera, both quarter and full wave retardation plates, and a Mettler Model FP82HT hot stage was used to collect digital images of RDX and HMX samples (2-3 mg). The stage had a 30 mm² window and viewing area of ~10 mm². Images were captured at the highest resolution in 15-second intervals, with the first picture at ambient temperature; samples were heated from 190°C to 205°C (1°C/minute) with camera views refreshed every second. At 205°C, heat was turned off, and the sample cooled.

Results and Discussion:

A number of experiments, reported herein, showed that Holston RDX lots contained detectable amounts of HMX, while the Dyno Nobel and Eurenco RDX did not. The total ion current (TIC) chromatograms obtained by mass spectrometry using a direct insertion probe showed the samples of Dyno Nobel and Eurenco insensitive RDX (SI RDX) had a single peak between 1.7 and 2.0 minutes. The mass spectrum was consistent with RDX having mass/charge fragments at 42, 46, 56, 71, 75, 82, 98, 102, 112, 120, 128, 148, 157, 205, and 219 m/z. In contrast the TIC chromatograms of the baseline Holston RDX and the two re-processed Holston RDX lots (by Eurenco) included two peaks--the first between 1.7 and 2.0 minutes (RDX fragmentation pattern), and a second peak between 3.5 and 3.7 minutes. The latter peak had a fragment distribution consistent with HMX (42, 46, 56, 71, 75, 82, 98, 102, 112, 120, 128, 148, 157, 205, 219, 222, 256 and 264 m/z). Despite the re-crystallization of the two Holston RDX lots by Eurenco, some HMX remained detectable in the samples. X-ray diffraction

(XRD), Raman, or infrared (IR) spectroscopy easily differentiated between pure RDX and pure HMX by visual comparison of their spectra. The baseline samples indicated that the Holston samples are differentiated from pure RDX by the presence of HMX. The techniques did not provide evidence of a different polymorphic distribution.

The HMX and RDX in Holston RDX were well resolved by high-performance liquid chromatography (HPLC) with retention times of 2.5 minutes and 4.0 minutes, respectively. Quantification of HMX was obtained using standard curves with nitrobenzene as an internal standard. Table 3 shows the percentages of HMX determined in the baseline samples and in samples aged at 60°C for one year. The RDX aged for one year at 60°C showed an apparent increase in HMX relative to RDX content. Decomposition of RDX to form HMX has not been observed¹ even for RDX low temperature decomposition.² However, to test the possibility that the aging of RDX increased HMX content relative to RDX, aliquots of Holston RDX, re-processed by Euroenco (lots 1 and 2), were heated just below the melting point (200°C) of RDX for various periods of time up to 200 minutes; these samples were subsequently analyzed by HPLC to quantify both RDX and HMX. The RDX was found to decompose faster than HMX at 200°C, (Figure 1) so that the ratio of HMX relative to RDX increased. Instead of a true increase in HMX content, a better explanation for results in Table 3 is variability in HMX content in different barrels of the reprocessed RDX returning from Euroenco (there have been some reports to that effect³).

The data above differentiates the samples by HMX content. Data acquired by IR, Raman, MS, or HPLC analyses showed the least sensitive RDX samples, SI-RDX and Dyno Nobel RDX, exhibited no or only traces of HMX, even upon 60°C aging. Comparing Tables 1 and 3 it appears that the most sensitive formulations, in terms of the large-scale gap test, contained the most HMX. Differential scanning calorimetry (DSC) proved the most useful technique for observing the differences among RDX lots. The DSC thermographs of RDX and HMX are distinctly different. RDX exhibited a melting

endotherm around 204°C and an exotherm immediately thereafter centered at 249°C; while HMX had a melting endotherm centered at 280°C followed by an exotherm at 286°C (Figures 2 and 3). All five baseline samples exhibited predominantly RDX features, and no significant differences were observed from examinations of their exothermic maxima (shown in Table 4 in replicate). However, in some of the samples, a second endothermic event at or near 190°C was observed. This feature was present in the unrefined Holston sample (H RDX) and both the reprocessed Holston samples (HI RDX-2 and HI RDX-1) (Figure 4). This endotherm was not observed in SI RDX or Dyno Nobel RDX (Figure 5), unless these samples were spiked with about 10% HMX. We and others attribute the early endotherm to an RDX/HMX eutectic^{4,7} although the possibility of low-temperature decomposition products cannot be dismissed. McKenney and Krawietz⁴ correlated the melting temperature of RDX to HMX content.

The aged samples of RDX (one year at 60°C or ambient temperature) were examined by DSC. Dyno Nobel RDX and SI RDX gave DSC thermographs similar to those of the baseline samples, but the three Holston samples exhibited a marked increase in the size of the endotherm near 190°C (Figure 6). The increase in the size of this feature in the unrefined Holston sample (H RDX) was large enough to obscure the melting endotherm observed in the thermographs of the baseline sample (Figure 7).

To examine the effect of heating RDX near its melting point, several DSC experiments were performed. RDX samples were thermally cycled three times from an elevated temperature to -20°C, with holds at the temperature extremes of one-half hour. Elevated temperatures of 80°C, 190°C, and 200°C were used. Upon cycling to 80°C, the thermographs of the re-processed Holston samples (lots 1 and 2) and the un-reprocessed Holston sample exhibited noticeable increases in the prominence of the endothermic feature near 190°C. Enhancement of this endotherm was not observed in the HMX-free Dyno Nobel or SIRDX samples. When the upper temperature was 190°C, the subsequent DSC scan appeared little different from that of the samples cycled up to 80°C, with the exception that the second exothermic peak was markedly larger than the first (Figure 8). (In the baseline samples of RDX, the

second exothermic peak appeared only as a slight shoulder on the main exotherm). In the samples cycled to 190°C, the first exothermic peak has decreased so much in height that the second endotherm was about the same height. This is consistent with results observed during isothermal heating at 200°C: RDX decomposed faster than HMX. The increases in relative HMX content could contribute to the formation of the RDX/HMX eutectic. When reprocessed Holston RDX (lots 1 and 2) were thermally cycled three times to 200°C no DSC peaks were detected. This was interpreted as complete decomposition of the RDX samples. RDX samples held at 200°C for shorter periods of time (i.e. 24 minutes) and subsequently cooled and scanned showed an endotherm about 171°C and a small exotherm at about 201°C before the major exotherm with two peaks at 243°C (RDX) and 255°C (HMX) (Figure 9). We interpreted this to mean that intermediate decomposition products formed to create a new low-temperature eutectic and a less thermally stable mixture.

A Nikon Eclipse 400 Pol polarized-light microscope equipped with a Mettler Toledo FP82HT hot stage was used to observe changes in morphology of the RDX samples rapidly equilibrated at 190°C and then heated at 1°C per minute to 205°C. Over the range of heating, pure HMX did not melt. Pure RDX (SIRDX) melted, but rapidly recrystallized upon cooling. Holston RDX, containing HMX contaminant, melted over the 190°C to 205°C range; however, it did not completely re-crystallize upon cooling. When samples of SIRDX and HMX were placed in contact, side-by-side on a microscope slide melting initiated at the RDX side of the boundary at 190°C. As the temperature was increased from 190°C to 205°C at 1°C per minute, the liquid RDX rapidly spread across the boundary and incorporated the solid HMX. By 205°C, the entire sample was melted, but when cooled back to ambient temperature, some of the material did not recrystallize.

The studies reported above were performed with the unformulated RDX, i.e. no binder; while the gap tests, by which sensitivities were evaluated, were performed on formulated materials. Samples of

plasticized RDX explosive (PAX/AFX 194) were examined by DSC. The one distinguishable difference between the thermographs of PAX/AFX 194 and the parent crystalline RDX was an endotherm centered at 80°C. This feature was attributed to the plasticizers (dioctyl adipate, carnauba wax, and ozokerite wax). The thermographs of PAX/AFX 194 formulated from SIRDX were very similar to the thermographs of neat SIRDX: an endotherm at 204°C and an exotherm near 250°C. However, the thermograph of PAX/AFX 194 formulated from Dyno Nobel RDX showed an endotherm near 190°C, even though the thermographs of the crystalline RDX from Dyno Nobel aged for one year did not develop this second endotherm (Figures 10 and 11). The 190°C endotherm was present in the thermographs of all the PAX/AFX 194 formulated from the Holston samples. In the thermograph of PAX/AFX 194 formulated from the unrefined Holston RDX, the 190°C endotherm was barely resolved from the melt endotherm, while in the thermographs of PAX/AFX 194 formulated from reprocessed Holston RDX, the endotherm near 190°C was so large that it completely obscured the melt endotherm.

The reprocessed Holston RDX lots 1 and 2 were initially insensitive (i.e. gap test 42-43 kbar); they only became sensitive after accelerated aging at 60°C or after sitting for months at ambient temperature. In evaluating the reason aging might affect the formulated RDX, the 190°C RDX/HMX eutectic must be considered. Isothermal heating of reprocessed Holston RDX at 200°C showed that RDX was lost faster than HMX (Figure 1) so that the ratio of HMX relative to RDX increases. Instead of a true increase in HMX content, a better explanation for results in Table 3 is variability in HMX content in different barrels of the reprocessed RDX returning from Euroenco.⁸ Even if HMX content does not actually increase with age, it is possible that the RDX/HMX eutectic does. This study showed that thermal cycling up to 80°C increased the size of the 190°C eutectic in the unformulated RDX samples that initially contained some nominal amount of HMX. Since in the unformulated RDX the eutectic can be detected after relatively low-temperature heating (up to 80°C), it is possible that the presence of plasticizers and binders might enhance mobility sufficiently that the RDX/HMX eutectic increases over

time under ambient conditions. This hypothesis seemed to be confirmed by the observation that while the unformulated Dyno Nobel RDX exhibited no low temperature eutectic, even after one year of heating at 60°C, the same material formulated as PAX/AFX 194 showed a eutectic region in the DSC scan after storage one year at ambient conditions. Thus, it appeared that the presence of the RDX/HMX eutectic, rather than strictly the HMX content, enhanced sensitivity to the large-scale gap test. The formation of the eutectic at storage temperatures requires the presence of a minimum amount of HMX and a mobilizing agent.

Conclusions:

Sensitivity on the large-scale gap test correlates with the HMX content of the RDX and the age of the formulation. SI RDX and Dyno Nobel RDX achieve insensitivity by almost complete absence of HMX. Freshly formulated samples of reprocessed Holston RDX are also insensitive as is freshly made PAX/AFX formulations made with aged, reprocessed Holston RDX. RDX, containing sufficient amount of HMX, over time, with the aid of mobilizing agents (polymer/binder ingredients), forms a RDX/HMX eutectic (190°C) which sensitizes the formulation. Such “re-sensitization” was observed with as little as 2% HMX in the RDX, which had been formulated and aged in the binder matrix. Formation of an RDX/HMX eutectic near 190°C has been previously reported, but not with less than 17% HMX.^{1,2} Although in DSC, this eutectic is not visible until 190°C, due to the conversions observed in the samples which had been thermally cycled to 80°C and in samples aged at 60°C, it appeared the eutectic can be obtained at even lower temperature. In fact, it seemed the plasticizer enhanced the conversion. The PAX/AFX 194 made with Dyno Nobel RDX exhibited a 190°C eutectic after a year of storage at ambient conditions even though the unformulated RDX did not show this feature.

Acknowledgements:

The authors wish to thank researchers at Picatinny Arsenal for funding this work.

References:

1. R. Behrens and S. Bulusu, Thermal decomposition of energetic materials. 2. Deuterium isotope effects and isotopic scrambling in condensed-phase decomposition of octahydro-1,3,5,7-tetranitro-1,3,5,7-tetrazocine, *J. Phys. Chem.*, 95, 5838-5845 (1991); R. Behrens and S. Bulusu, Thermal decomposition of energetic materials. 3. Temporal behaviors of the rates of formation of the gaseous pyrolysis products from condensed-phase decomposition of 1,3,5-trinitrohexahydro-s-triazine (RDX), *J. Phys. Chem.*, 96, 8877-8891(1992); R. Behrens and S. Bulusu, Thermal decomposition of energetic materials. 4. Deuterium isotope effects and isotopic scrambling (H/D, ¹³C/¹⁸O, ¹⁴N/¹⁵N) in condensed-phase decomposition of 1,3,5-trinitrohexahydro-s-triazine (RDX). *J. Phys. Chem.*, 96, 8891-8897(1992); J.C.Oxley, A.Kooh, R.Szeckeres, W.Zheng, Mechanisms of Nitramine Thermolysis, *J. Phys. Chem.*, 98, 7004-7008 (1994)
2. S. Maharrey; R. Behrens, Thermal Decomposition of Energetic Materials. 5. Reaction Processes of 1,3,5-Trinitrohexahydro-s-triazine (RDX) Below Its Melting Point;” *J. Phys. Chem.* (in press).
3. Personal communications, S. Struck and B. Fishburn.
4. R.L. McKenney and T.R. Krawietz, Binary Phase Diagram Series: HMX/RDX, *J. Energetic Mater.* 21(3), 141-166 (2003).
5. L. Reich, Melting and decomposition of RDX-HMX [cyclotrimethylene trinitramine-cyclotetramethylene tetranitramine] mixtures by DTA, *Thermochimica Acta* 7(1), 57-67 (1973).
6. R.D. Chapman and J.W. Fronabarger, A convenient correlation for prediction of binary eutectics involving organic explosives, *Propellants, Explosives, Pyrotechnics* 23(1), 50-55 (1998).
7. J.R. Quintana, J.A. Ciller and F.J. Serna, Thermal behavior of HMX/RDX mixtures, *Propellants, Explosives, Pyrotechnics*, 17(3), 106-9 (1992).

List of Tables

Table 1: Large-Scale Gap Test on Baseline and Aged (60°C) Samples (the lower the pressure, the more sensitive the RDX)

Table 2: Baseline RDX Samples

Table 3: Percentage of HMX in Baseline and Aged RDX

Table 4: DSC of RDX Samples at Various Scan Rates

Table 1: Large-Scale Gap Test on Baseline and Aged (60°C) Samples
(the lower the pressure, the more sensitive the RDX)

RDX sample	baseline	60C
	k bars	kbars
SIRDX	46.3	46.0
Dyno Nobel	44.3	45.2
Holston # 1	43.4	39.2
Holston # 2	41.6	29.1
Holston	35.6	34.7

Table 2: Baseline RDX Samples

SI RDX		Insensitive RDX from SNPE (Eurengo)
DN RDX		Insensitive RDX from Dyno Nobel
H RDX	93k517-041	Holston RDX made about 1994
HI RDX-1	0800s00	Holston RDX reprocessed Dec 2000 (lot 1)
HI RDX-2	2715s-2	Holston RDX reprocessed Jan 2002 (lot 2)

Table 3: Percentage of HMX in Baseline and Aged RDX

	baseline	60°C	
		6 mon	1 yr
SI RDX	0.0%	0.0%	0.1%
Dyno Nobel	0.1%	0.2%	0.1%
Holston #1	2.9%	6.6%	5.4%
Holston #2	1.9%	6.9%	4.7%
Holston	15.5%	14.5%	15.6%

Table 4: DSC of RDX Samples at Various Scan Rates

Sample Name	Scan Rate 20°C/min				Scan Rate 10°C/min				Scan Rate 5°C/min				Scan Rate 1°C/min			
	Endotherm °C	Heat (J/g)	Exotherm °C	Heat (J/g)	Endotherm °C	Heat (J/g)	Exothe m °C	Heat (J/g)	Endotherm °C	Heat (J/g)	Exother m °C	Heat (J/g)	Endotherm °C	Heat (J/g)	Exotherm °C	Heat (J/g)
SIRDX	208	46	254	3542	206	134	242	4796								
	206	51	253	2503	206	167	242	4913								
Dyno Nobel	207	136	250	5257	202	133	242	3706	204	95	239	4370	204	87	240	3327
	207	142	252	4902	200	114	241	4434					201	55	220	4158
Holston 0800s00	205	37	253	3008												
lot 1	208	54	257	1519												
Holston 2715s02	208	83	250	4515	203	87	241	4719	202	53	238	4486	not det.	not det.	219	3520
lot 2	207	149	256	2785	202	172	248	10507	201	54	240	2770	191	55	220	3542
Holston 93k517-041	207	142	249	6079	205	105	247	2533	189	66	244	3693	188	39	222	3982
un-reprocessed	206	91	249	5280					192	30	242	3663	186	49	221	4288

List of Figures

Figure 1. HPLC Analysis of Remaining RDX (Holston, lot 1) and HMX during 200°C Thermolysis

Figure 2. DSC Thermograph of RDX (SIRDX)

Figure 3. DSC Thermograph of HMX

Figure 4. DSC Thermograph of RDX (Holston, lot 2) with expansion of endothermic region

Figure 5. DSC Thermograph of RDX (Dyno Nobel) with expansion of endothermic region

Figure 6. DSC Thermograph of RDX (Holston, lot 2): top (baseline) & upon aging at 60°C, middle (6 mon), bottom (1 yr)

Figure 7. DSC Thermograph of RDX (Holston): top (baseline) & upon aging at 60°C, middle (6 mon), bottom (1 yr)

Figure 8. DSC Thermograph of RDX (Holston, lot 1) thermally cycled 190°C to -20°C three times, held at extremes 30 min.

Figure 9. DSC Thermograph of RDX (Holston, lot 1) heat 24 minutes at 200°C prior to DSC scan at 20°/minute

Figure 10. DSC Thermograph of RDX (DynoNobel) formulated as PAX/AFX 194 aged one year at ambient conditions

Figure 11. DSC Thermograph of RDX (DynoNobel) aged one year at 60°C.

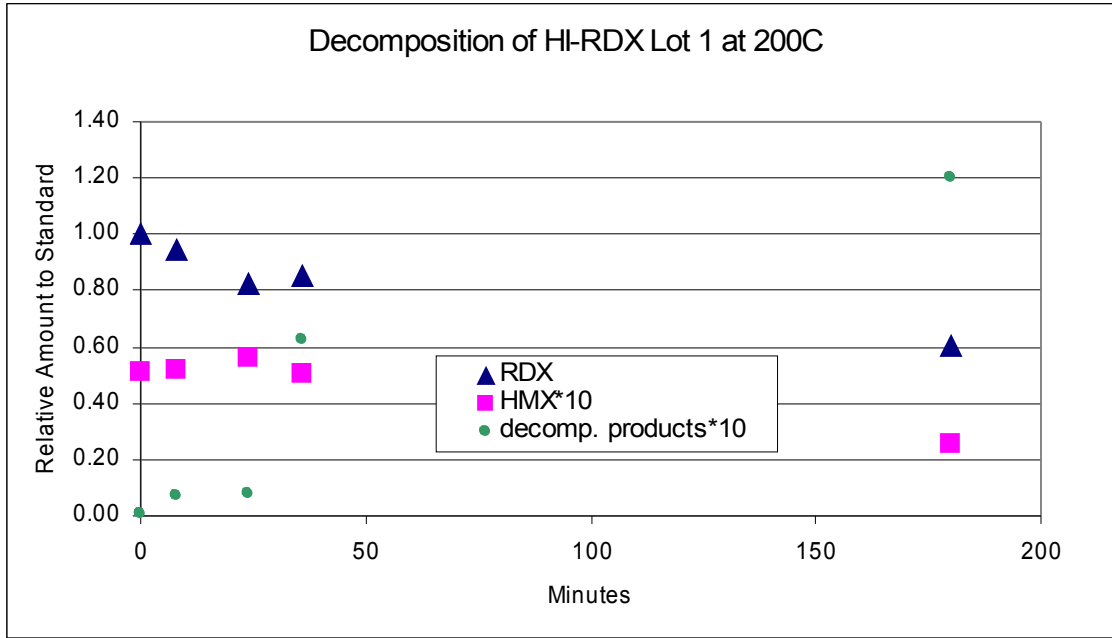


Figure 1. HPLC Analysis of Remaining RDX (Holston, lot 1) and HMX during 200°C Thermolysis

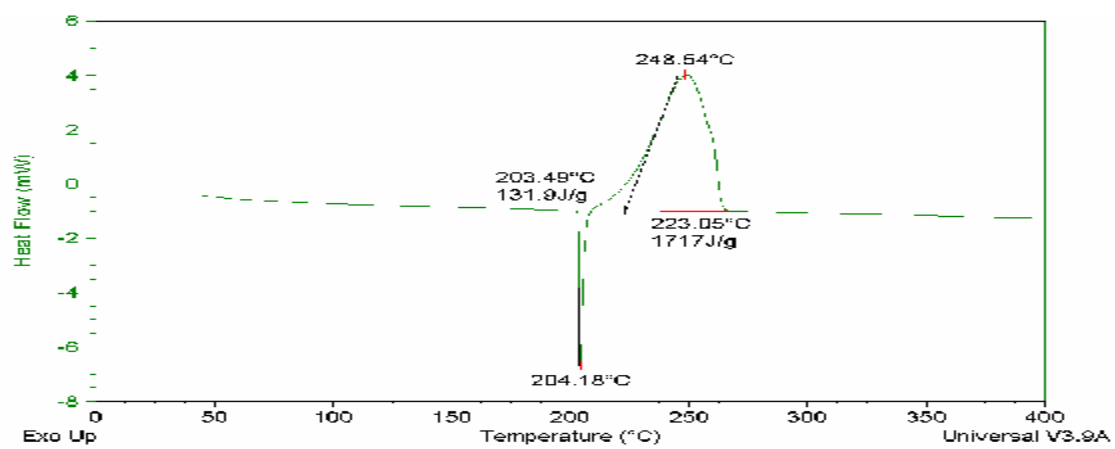


Figure 2. DSC Thermograph of RDX (SIRDX)

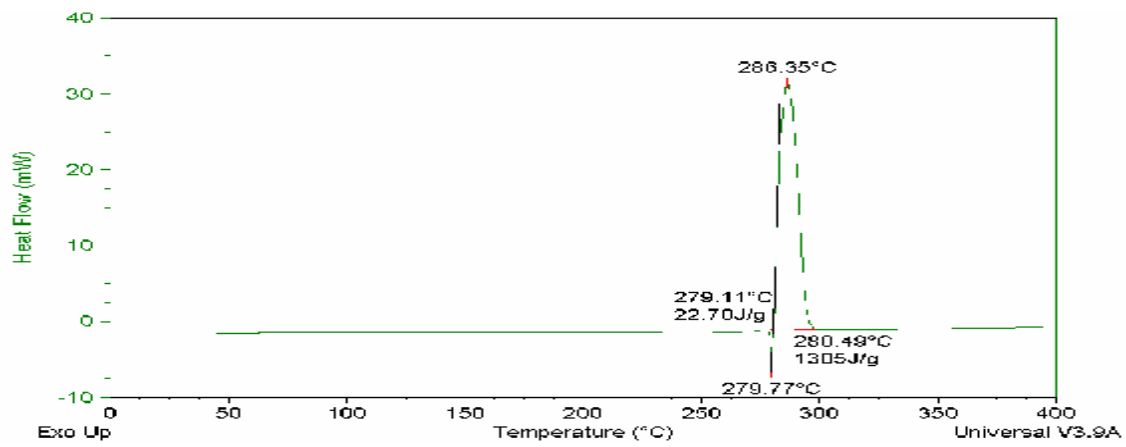


Figure 3. DSC Thermograph of HMX

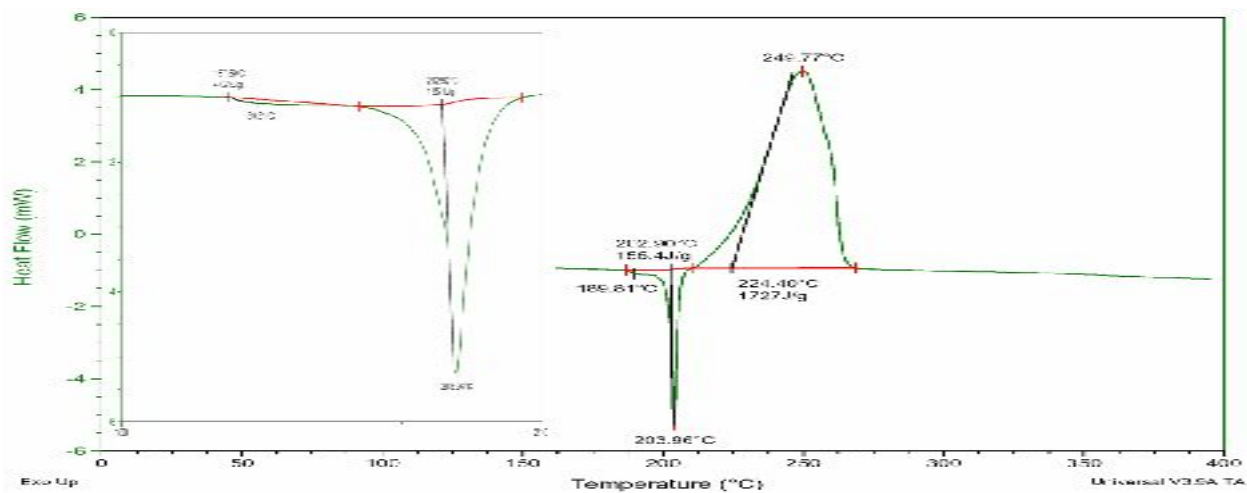


Figure 4. DSC Thermograph of RDX (Holston, lot 2) with expansion of endothermic region

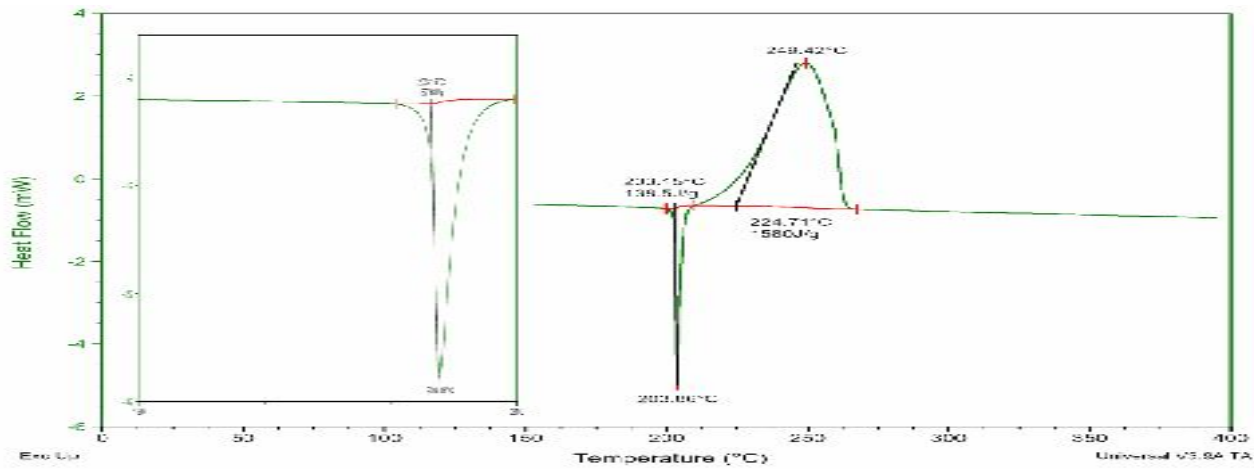


Figure 5. DSC Thermograph of RDX (Dyno Nobel) with expansion of endothermic region

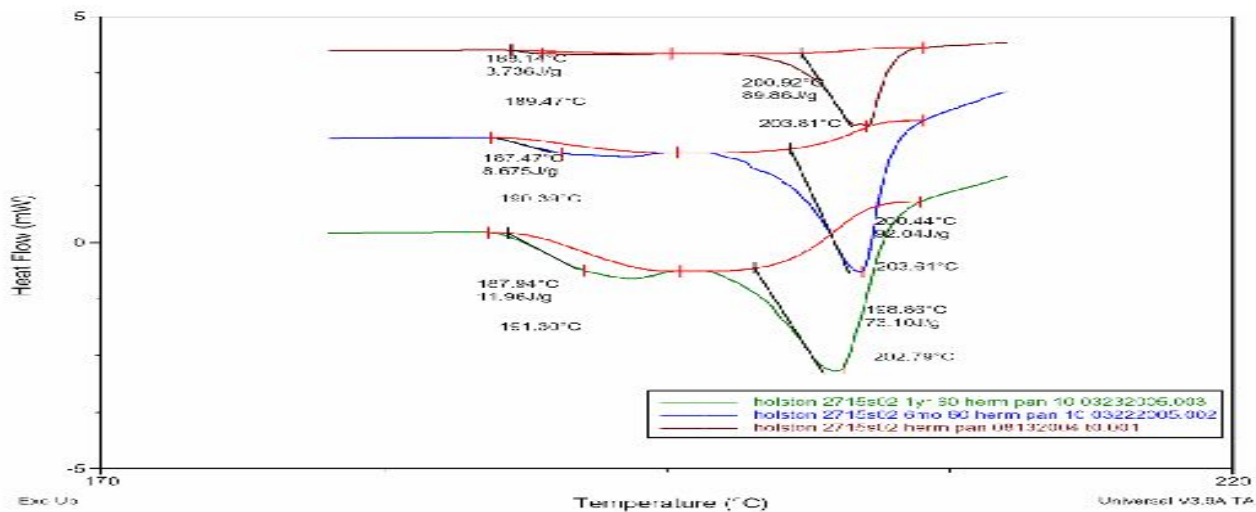


Figure 6. DSC Thermograph of RDX (Holston, lot 2): top (baseline) & upon aging at 60°C, middle (6 mon), bottom (1 yr)

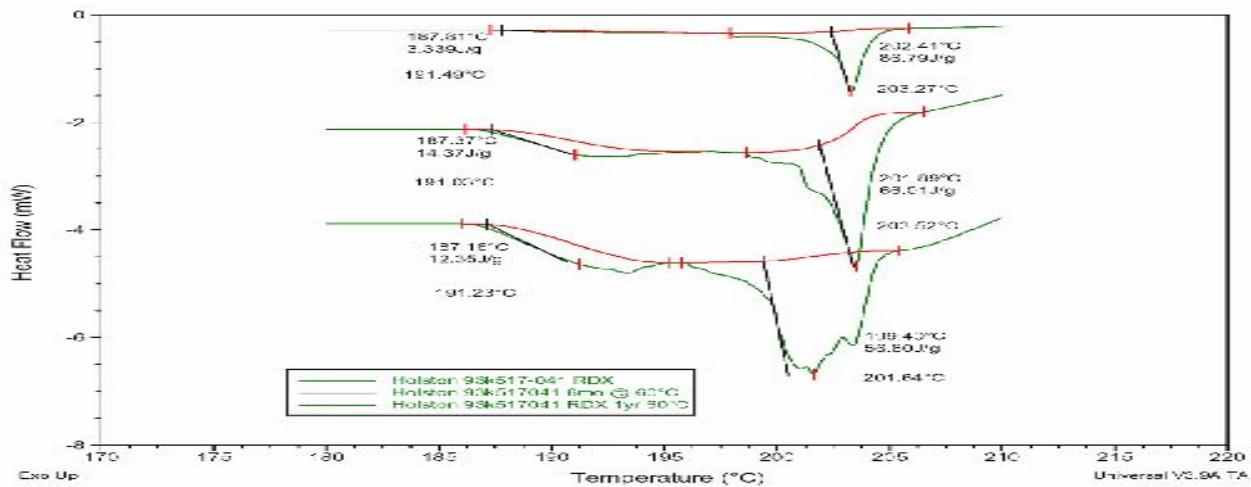


Figure 7. DSC Thermograph of RDX (Holston): top (baseline) & upon aging at 60°C, middle (6 mon), bottom (1 yr)

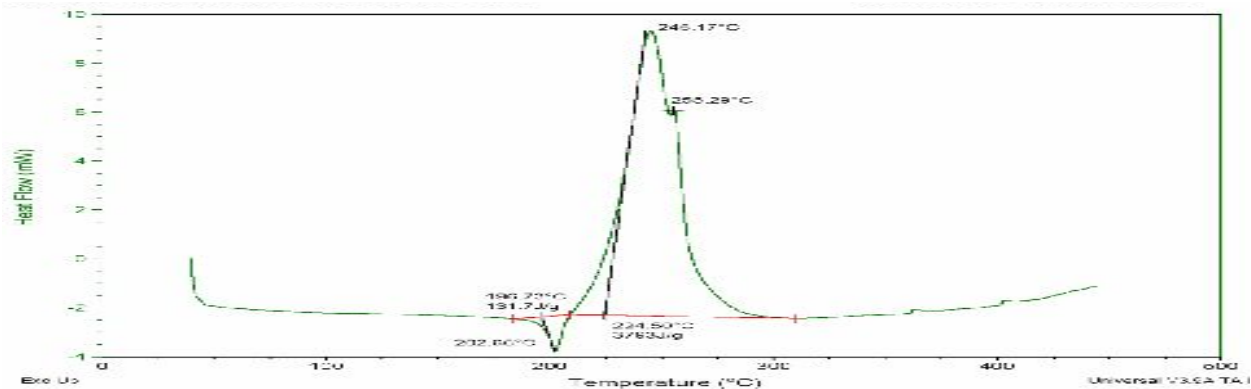


Figure 8. DSC Thermograph of RDX (Holston, lot 1) thermally cycled 190°C to -20°C three times, held at extremes 30 min.

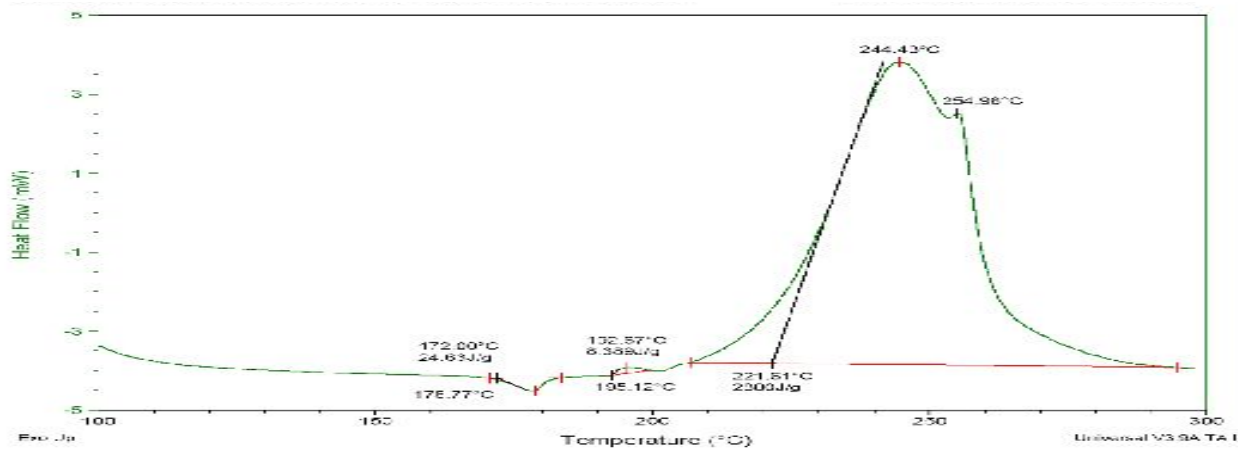


Figure 9. DSC Thermograph of RDX (Holston, lot 1) heat 24 minutes at 200°C prior to DSC scan at 20°/minute

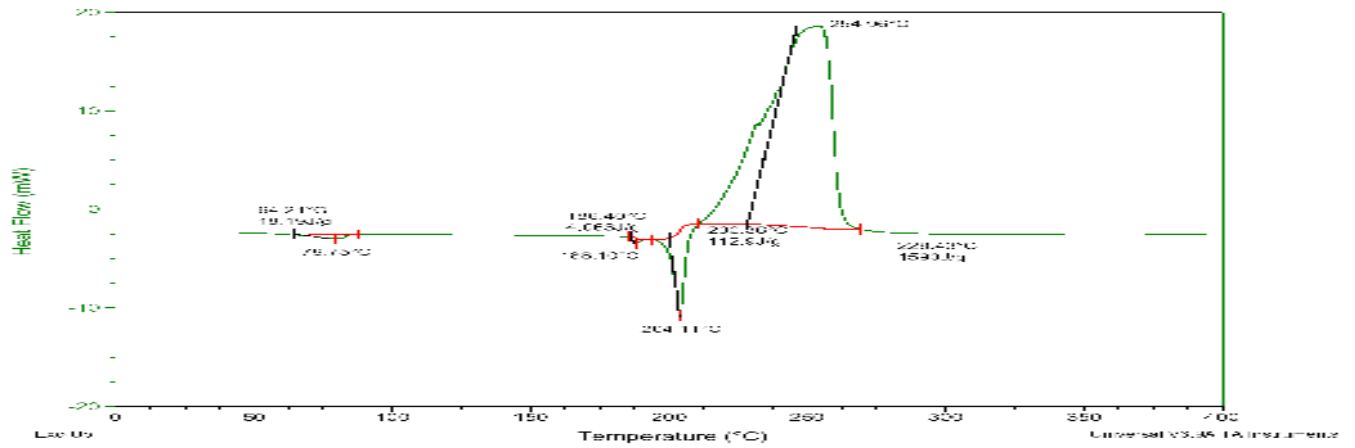


Figure 10. DSC Thermograph of RDX (DynoNobel) formulated as PAX/AFX 194 aged one year at ambient conditions

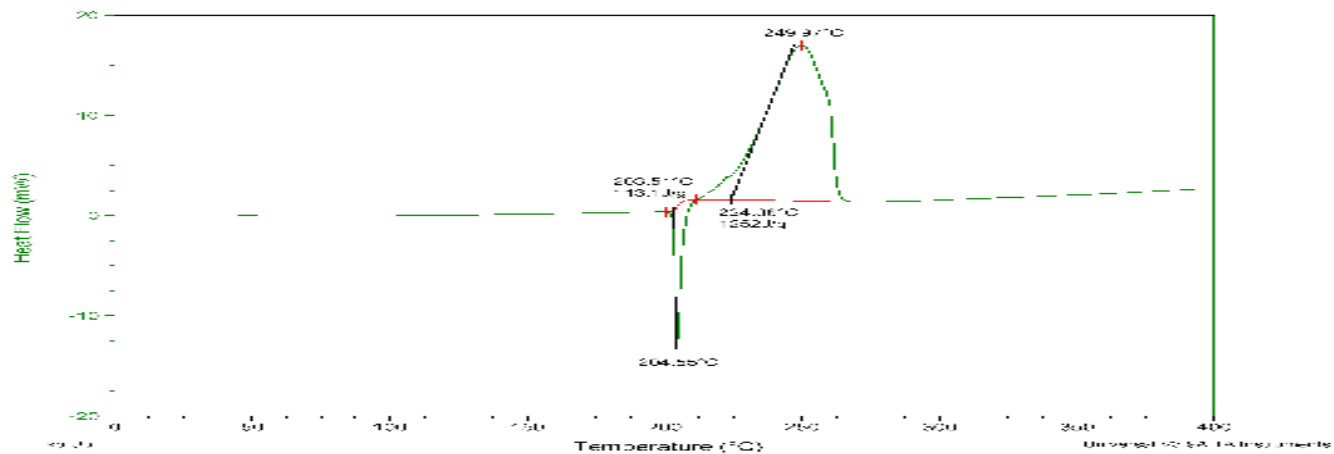


Figure 11. DSC Thermograph of RDX (DynoNobel) aged one year at 60°C